Ankle-Knee Prosthesis with Active Ankle and Energy Transfer: Development of the CYBERLEGs Alpha-Prosthesis

Louis Flynn[a,*], Joost Geeroms[a], Rene Jimenez-Fabian[a], Bram Vanderborght[a], Nicola Vitiello[b,c], Dirk Lefeber[a]

[a] *Department of Mechanical Engineering, Vrije Universiteit Brussel, Pleinlaan 2, Brussels, Belgium*
[b] *The BioRobotics Institute, Scuola Superiore Sant'Anna, viale Rinaldo Piaggio 34, Pisa, Italy*
[c] *Don Carlo Gnocchi Foundation, via di Scandicci 256, 50143, Firenze, Italy*

Abstract

This paper presents the development of the CYBERLEGs Alpha-Prototype prosthesis, a new transfemoral prosthesis incorporating a new variable stiffness ankle actuator based on the MACCEPA architecture, a passive knee with two locking mechanisms, and an energy transfer mechanism that harvests negative work from the knee and delivers it to the ankle to assist pushoff. The CYBERLEGs Alpha-Prosthesis is part of the CYBERLEGs FP7-ICT project, which combines a prosthesis system to replace a lost limb in parallel with an exoskeleton to assist the sound leg, and sensory array to control both systems. The prosthesis attempts to produce a natural level ground walking gait that approximates the joint torques and kinematics of a non-amputee while maintaining compliant joints, which has the potential to decrease impulsive losses, and ultimately reduce the end user energy consumption. This first prototype consists of a passive knee and an active ankle which are energetically coupled to reduce the total power consumption of the device. Here we present simulations of the actuation system of the ankle and the passive behavior of the knee module with and without the energy transfer effects, the mechanical design of the prosthesis, and empirical results from testing of the

☆A preliminary version of this paper was presented at the Wearable Robotics Workshop, Neurotechnix 2013.

*Corresponding author

Email addresses: lflynn@vub.ac.be (Louis Flynn), jgeeroms@vub.ac.be (Joost Geeroms), rjimenez@vub.ac.be (Rene Jimenez-Fabian), bram.vanderborght@vub.ac.be (Bram Vanderborght), n.vitiello@sssup.it (Nicola Vitiello), dlefeber@vub.ac.be (Dirk Lefeber)

physical device with amputee subjects.

Keywords: Prosthesis, Knee, Ankle, Energy Efficiency, Transfemoral, CYBERLEGs, Active, Energy Transfer

1. Introduction

The number of people who have undergone a lower limb amputation has risen worldwide during the recent decades [1], victims of cardiovascular diseases, trauma, malignancy, or congenital limb defects. In developed countries, this increase is primarily attributed to a rise in vascular diseases, particularly diabetes related amputations, where a higher activity level and faster recovery of mobility may be helpful to maintain health of the patient [2]. This recovery is impeded by the large efforts needed to use conventional prostheses, both physically and cognitively, at a time when the patient is most weak. The increased metabolic costs, increased forces, and abnormal gait kinematics associated with using standard passive prostheses are well known (for example [3, 4, 5, 6]) and make it difficult for weaker individuals to use passive prostheses. The CYBERLEGs FP7-ICT [1] project looks to solve this problem through the use of an active prosthesis, the topic of this paper, paired with an active orthotic exoskeleton being developed concurrently. It is believed that the complete system will be able to reduce the metabolic and cognitive costs of performing actions for the user of the system.

Recent years have seen the commercialization of a number of active prostheses designed to restore the full ankle [7, 8] and knee [9] joint capability during normal walking, as well as provide some slope walking, sit to stand, and stair climbing operations. In addition to the newest commercial models, there are a number of active ankle [10, 11, 12, 13] and knee modules [14], as well as combined ankle-knee systems [15]

[1] The CYBERnetic LowEr-Limb CoGnitive Ortho-prosthesis. The project aims for the development of an artificial cognitive ortho-prosthesis system for the replacement of the lost lower limb of dysvascular transfemoral amputees and to provide assistance to the remaining sound limb. The final prototype will allow the amputee to walk, use stairs and move from sit-to-stand and stand-to-sit with limited cognitive and energetic effort. www.cyberlegs.eu

under development, seeking to improve functionality and reduce energy consumption of both the device and the individual. These new devices have been spurred by developments in materials, electric motors, batteries, and miniaturized controllers, combined with actuators that are better suited to biomechanical use [16, 17, 18]. All of the modern ankle prostheses utilize some sort of passive compliance in their ankle designs. For example, the Vanderbilt prosthesis [15] uses a parallel spring in its ankle actuator to reduce the peak force required by the actuator to approximate normal gait torques, the SpringActive Odyssey [19] utilizes a series spring which it loads during stance and unloads during pushoff, and the BiOM [20] utilizes both to provide a combination of these effects. The AMP Foot 2.0 [10], developed at the Vrije Universiteit Brussel, uses a different combination of series spring systems and can explosively inject energy into the system using a four-bar linkage as a locking mechanism. Most importantly, some of these active prostheses have shown significant improvement in gait kinematics when compared to a passive prosthesis, and one powered ankle prosthesis has shown a metabolic energy performance equal to that of a normal walker [21]. It should also be noted that Herr and Grabowski of [21] speculate that with additional development it should be possible to reduce the metabolic cost of an amputee walking on level ground to below that of a non-amputee.

There are a growing number of existing active knee systems, but only the Ossur Power Knee [9] is commercially available on the market. Current knees in development include the MIT agonist-antagonist [14] and CSEA [22] knees, a screw driven knee from University of Sakarya [23], and Hebei University of Technology [24]. The Vanderbilt knee-ankle prosthesis is currently the only tested, active, combined ankle-knee prosthesis in the research stages of development [15]. The knee design of [15] is a rigid actuation model, where the joint has no intrinsic series or parallel compliance. The Power Knee [9] has a stiff spring in series with the drive motor, and the MIT knees also utilize compliant systems in their actuation.

Most prosthetic devices treat the knee and ankle as separate systems for commercial benefits and simplicity of design, while in humans there are clear connections between joints through biarticular muscles. The CYBERLEGs Alpha-Prosthesis attempts to recreate these types of connections between the knee and ankle in an active prosthesis.

Because the knee performs primarily negative work during normal walking, the energy that would normally be dissipated can be used for powering pushoff. Although not common, there are a few passive designs that have attempted knee and ankle energy transfer. For example the HydraCadence [25] from the 1950's (and still available today) utilizes a passive hydraulic system that uses knee flexion during swing phase to provide ankle dorsiflexion, effectively transferring energy from the knee to the ankle, but not providing high levels of work and providing no additional energy to the ankle during pushoff. Designs of VUB HEKTA [26] and the University of Twente [27] passively transfer energy that would be dissipated by the knee (13J for an 80kg person), to the ankle through thoughtful use of mechanical linkages and springs. This is beneficial since the ankle requires around 18J during pushoff. This concept of energy transfer between joints has not yet been incorporated into active designs.

The CYBERLEGs Alpha-Prosthesis is a new knee-ankle system consisting of an active ankle and passive knee, paired with a novel energy transfer system between the knee and the ankle. The system is designed to be able to closely reproduce the full normal gait joint torques for an 80kg person during normal walking at a lower electrical cost than a directly driven prosthetic system. The actuated ankle is a new, highly compliant, MACCEPA-based [28], variable stiffness actuator capable of providing positive net work. The knee consists of two springs, one of which can be activated using a small servomotor, to passively approximate the torque-angle characteristics. The energy transfer system is a cable that is locked and unlocked with a second small servomotor, directly coupling the knee and ankle during specific times in the gait cycle. The components were then characterized and tested with sound patients using a bent-knee cast and finally used in amputee trials. Here we present the simulation of both the ankle and the knee, mechanical design decisions that were made based on the simulations, initial tests of the CYBERLEGs Alpha-Prosthesis, and discussion and comparison of the behavior of the new system as an integral part of the CYBERLEGs FP7-ICT project.

2. Theory of Operation

During normal walking the ankle needs to produce around $18J$ positive work per stride. This can be provided through the use of a powered prosthesis, but directly coupling a drive to the joint output requires motors that can provide over $300W$ and torques of around $130Nm$. The power requirement of an actuated ankle can be greatly reduced through the use of a Series-Elastic Actuator (SEA) [29] because the work needed for ankle push off can be injected over a longer time and stored in the elastic element until used, which is not possible in a directly driven system.

The knee, on the other hand, has a net braking effect, needing to dissipate around $13J$ per step. This energy is generally dissipated in current state of the art prostheses through the use of a passive damper, such as the Mauch knee [9], or in an active microprocessor controlled damper, such as the C-Leg [30] or Rheo [9] knees. In the Alpha-Prosthesis, the energy is stored in springs to be used at different times during the gait cycle. Through the use of a connection between the knee and the ankle, it becomes energetically interesting to capture the excess work at the knee because it can be used to power the ankle. The major issue is that the negative work at the knee does not always coincide with the times the ankle needs the most energy and therefore the knee needs a method to store and release energy at the correct time, necessitating the use of a locking mechanism.

Here we present the theory and simulation of the ankle and knee systems independently, and finally in combination with the energy transfer mechanism.

2.1. Ankle

During level ground walking, the ankle joint requires a positive joint work of approximately $18J$ per step for an $80kg$ individual walking at $1stride/second$. It is first assumed that this energy will be provided solely through a MACCEPA based actuator, a variable compliance, series elastic actuator well suited for biologically inspired robots [28, 18]. A schematic of the design can be found in Figure 1 and the corresponding realization of the design can be found in Figure 11 in Section 3.1. This architecture was chosen not only because of the overall behavior of the system, but also to solve

some practical problems with previous designs, such as the ability to use compression springs and to remove cables which had been a point of failure of previous designs.

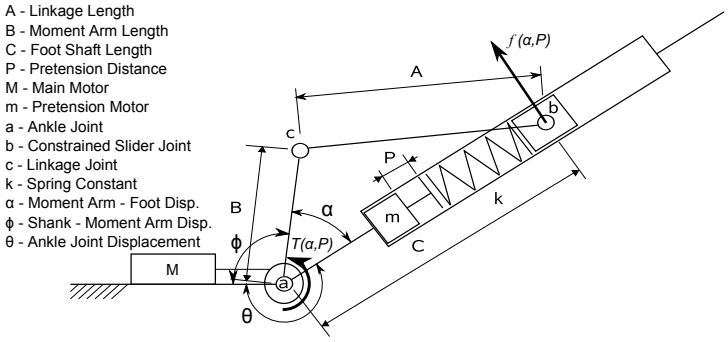

Figure 1: Configuration of a MACCEPA using rigid linkages. The main motor (M) is attached to the anchored link and drives the moment arm (b) around the ankle joint (a). The moment arm is displaced by an angle α, compressing the MACCEPA spring along the foot shaft (C), creating an ankle torque. The small motor (m) is used to precompress the main spring, and is attached to the foot link. Technical realization in Figure 11.

In this schematic the anchored segment represents the shank of the leg, and the main motor M drives the moment arm B around joint a. This motion pulls the linkage A, driving the linearly constrained slider b and compressing the spring k. The torque generated by the actuator is then dependent on only the displacement α and the initial spring pretension P, which is determined by the pretension motor (m).

The output torque developed by the actuator is given by

$$T(\alpha,P) = C(\alpha) f(\alpha,P) \tag{1}$$

Which is the product of the distance along the foot shaft, C, defined as

$$C(\alpha) = B\cos\alpha + A\left[1-\left(\frac{B}{A}\sin\alpha\right)^2\right]^{1/2} \tag{2}$$

and the perpendicular force to the foot shaft, $f(\alpha,P)$, defined as

$$f(\alpha,P) = \frac{kB(P+A+B-C(\alpha))\sin\alpha}{A\left[1-\left(\frac{B}{A}\sin\alpha\right)^2\right]^{1/2}} \tag{3}$$

where $f(\alpha,P)$ is the force acting on b perpendicular to $\overline{ab}$. Note that $B/A < 1$ should be satisfied to avoid a singularity at $\alpha = 90deg$.

As the displacement of the moment arm becomes larger the actuator naturally stiffens, which is similar to the natural behavior of the ankle. The torque of the joint can reach well over $130Nm$ and increases in stiffness from almost no stiffness around the neutral position, $\alpha = 0$, to around $15Nm/deg$ at high deflection and moderate ($9mm$) pretension, as can be seen in Figure 2. The selected final values used for the calculations, and eventually for the final design, can be found in Table 1. These values were determined through the following power simulations (Section 2.1.1) as well as the dimensional constraints for the foot actuator.

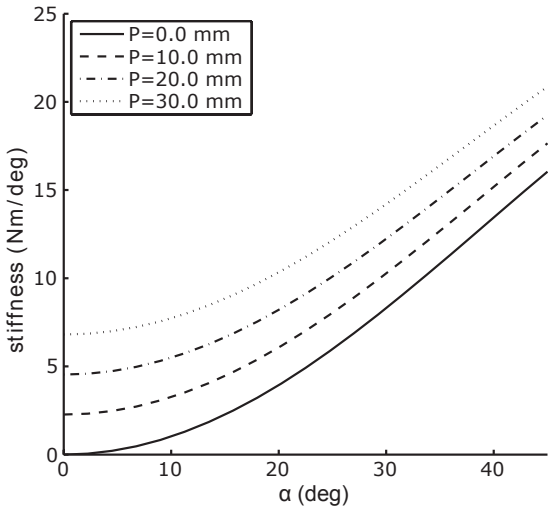

Figure 2: Ankle Stiffness in terms of α. The stiffness of the ankle joint automatically increases as the moment arm is displaced from the neutral position, as happens in a natural ankle.

2.1.1. Ankle Simulations

The ankle simulations are done in two parts, the first looks at the actuator output given the biomechanical data, and the second matches a motor to the requirements from the actuator.

To understand the actuator output requirements, desired torque, τ_{Winter}, and desired

Motors		
Property	Value	Units
Moment Arm Length (B)	10	mm
Linkage Length (A)	10	mm
Spring Constant (k)	130000	N/m
Shoe Size	42	EU
Gear Ratio	860:1	
Torque Output	130	Nm

Table 1: Selected Ankle Characteristics used in simulation and for final design.

ankle joint positions, θ_{Winter}, were determined from biomechanical data of healthy gait from Winter [31] assuming a $80kg$ individual walking at one stride per second. These were then used to calculate the required moment arm trajectory, in terms of α, at every moment in time over a single stride by solving the inverse of Equation 1, where $T(\alpha, P) = \tau_{Winter}$, the desired torque trajectory. Note that because the power of the output of the motor is the power to be optimized, the motion of the moment arm with respect to the shank, $\phi = \theta_{Winter} + \alpha$, with the offset where $\phi_0 = \theta_{Winter}0 = \alpha_0 = 0$, is used to calculate the moment arm velocity, shown in Equation 4. The definitions for the different angles α, ϕ, *and* θ can be found in Figure 1.

The shank referenced desired moment arm angle trajectory and velocity are then used to calculate required actuator output power, $T * \frac{d}{dt}(\phi)$. Because motor size is highly correlated with motor power, the spring constant and pretension length were optimized to minimize peak actuator power. The optimization problem is defined as

$$\underset{k,P}{argmin} \left[\underset{t_{stride}}{max} \left(\mid T * \frac{d}{dt}(\phi) \mid \right) \right] s.t. \begin{cases} 50000 < k < 250000\ N/m \\ 0 < P < 20\ mm \\ |\tau_{Winter} - T| < \delta \end{cases} \tag{4}$$

where T is the output joint torque of the actuator and t_{stride} is the time from initial heel contact to the end of the stride. A parameter substitution search, as was successfully used in [32], was performed to find local minimums in peak actuator power, given

the parameters of pretension distance, P, and MACCEPA series spring stiffness, k as shown in Figure 3. The step resolution of the pretension was $1mm$ and of the series spring stiffness was $10000N/m$.

The main MACCEPA spring constant was selected by choosing a spring that had a peak power minimum near the center of the the range of pretension that the device would be capable of producing (maximum pretension is around $20mm$), while keeping the peak power variation low over the entire pretension range. The ultimate spring constant that was used was determined by commercially available springs that fit the dimensions of the application.

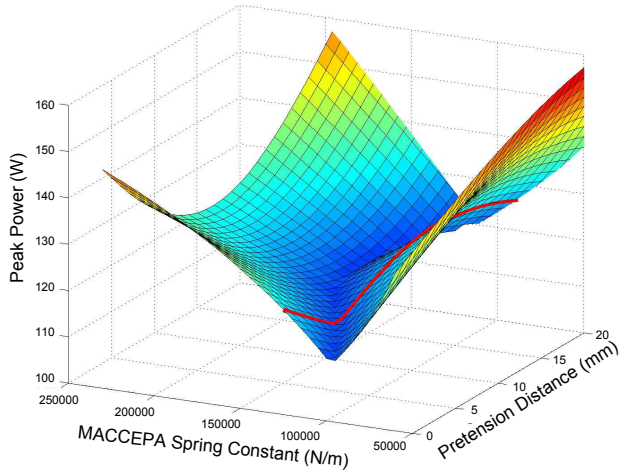

Figure 3: A surface showing the peak positive work of the actuator given the MACCEPA spring constant and pretension. The red line shows the path of the selected spring ($130000N/m$), with a minimum of $111W$ around $7mm$ pretension. The peak power requirement remains relatively low over the range of pretension that the ankle is able to produce.

Peak motor power was reduced from the $304W$ needed for a stiff direct drive system, to around $111W$. The power, torque, and position characteristics required to track the typical biological ankle torque with the MACCEPA actuator are shown in Figure 4. Note that increasing the pretension length increases the peak power slightly due to a change in the timing of the motion of the moment arm, but also dramatically reduces the required motor velocity, which has large implications for the selection of the motor.

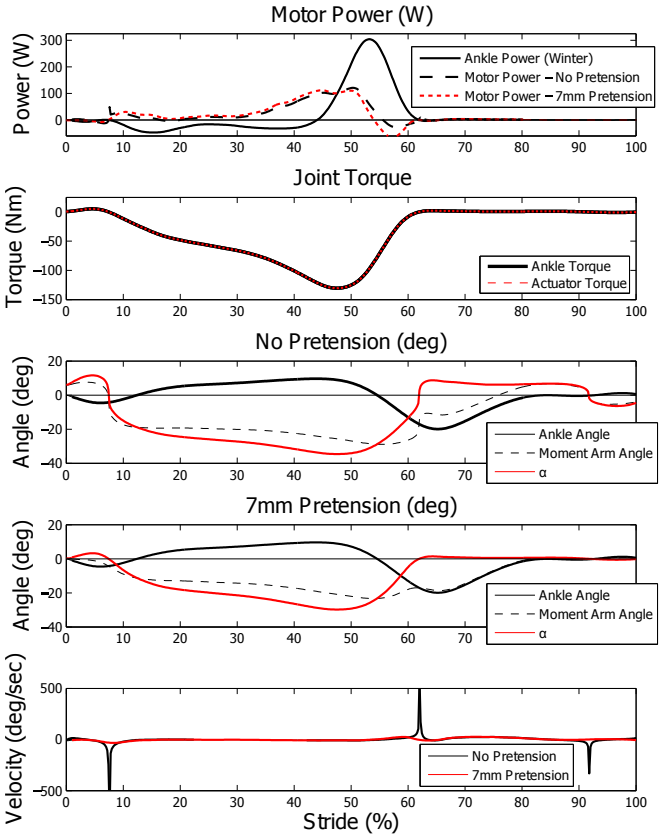

Figure 4: Power, torque and position characteristics of the ankle MACCEPA actuator tracking average normal gait characteristics. The power can be seen to be reduced from $304W$ to $111W$ in the first graph. The difference in peak power between no pretension and $7mm$ pretension is small (around $2W$). The output torque of the actuator matches the biological torque output exactly, due to the way the simulations are calculated. Although the difference in peak power is small, the difference in actuator velocity is very different in the no pretension and pretensioned conditions. In the same time, the angle varies from -35 to 10 degrees in the no pretension state, while it only needs to travel from -25 to 2 degrees in the pretensioned state. This is seen in the bottom frame where the peak velocity is reduced from over $500deg/sec$ to below $100deg/sec$ at $7mm$ pretension.

Using these moment arm trajectories and torque requirements, motor properties and gear ratios were selected. A Simulink model of the motor and MACCEPA actuator was created, using a controller similar to the system used in testing and in walking trials, as in Figure 5. The kinematics of the ankle joint and moment arm were commanded to track those of the Winter data and moment arm simulations from Figure 4 and the output torque was calculated. The torque of the actuator was determined for three different motor/gearbox combinations. The first was a high velocity system, with a high power motor ($200W$) and low gear ratio ($14:1$) gearbox. This is not an energy efficient system, but should be able to provide the best bandwidth, if the motor drivers can provide the current. The second is a high power motor, with a higher gearbox ratio ($86:1$). The third system was the one that was ultimately used in the prosthesis, a low power ($60W$) motor with a high ($86:1$) gearbox. Note that all of the combinations can reach torques within the standard deviation of the Winter ankle torque data.

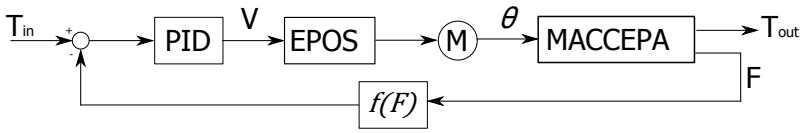

Figure 5: Controller for Matlab modeling and ankle torque testing. The moment arm position signal is fed through a PID controller to create a velocity setpoint for the EPOS controller. The EPOS drives the motor at the specified velocity, which compresses the main MACCEPA spring. The force on the spring is measured using a load cell and the output torque is calculated. At the same time the ankle joint is driven by another motor to track the Winter data.

For this method to produce torques and kinematics similar to a human gait, we must assume that our prosthesis has similar mass and inertia properties to the human leg otherwise it generates different dynamics, especially during the swing phase.

2.2. Knee

The knee is composed of three primarily passive components, the Baseline Spring (BL), the Weight Acceptance (WA), and the Energy Transfer (ET) systems. The combination of these three systems can create a torque-angle characteristic that mimics the natural torque-angle relationship of a normal knee. In the quasi-static analysis that has

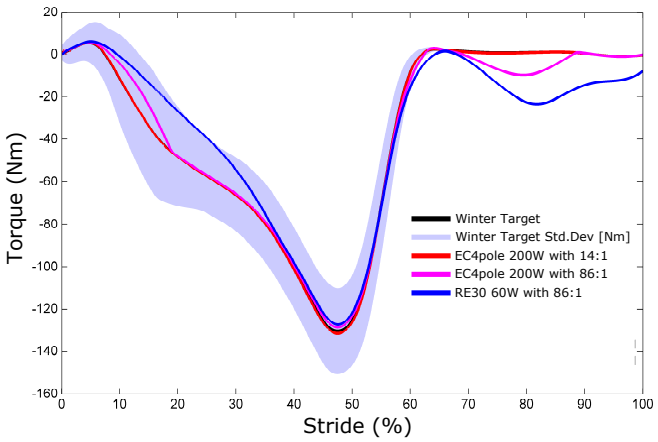

Figure 6: Simulink model results of three different motors tracking the torque of the ankle with a pretension of 7mm, using the kinematic position of the ankle and the desired moment arm position of the simulations from Figure 4. The effect of a lower bandwidth of the motor is shown by worse torque trajectory tracking. The three motor/gearbox combinations are, with exception of the swing phase, within the standard deviation of the Winter gait data [31], shown shaded in light blue.

been used for this prosthesis, the resultant torque of these three systems is the final knee torque, as in Equation 5.

$$T_k(WA_{Lock}, ET_{Lock}, \theta_k) = T_{WA}(WA_{Lock}, \theta_k) + T_{BL}(\theta_k) + T_{ET}(ET_{Lock}, \theta_k) \qquad (5)$$

where the total knee torque is dependent on the two (WA and ET) lock states, as well as the angle of the knee. Once again the goal of the system is to attempt to track the biological knee torque using a combination of these three mechanisms.

By examining the torque-angle characteristic of the knee, it can be shown that the knee normally dissipates energy, which provides the opportunity to harvest this energy to be used in another part of the prosthesis. Harvesting energy can be done by using springs for energy storage which can later be delivered to the ankle for assistance. The Alpha-Prosthesis has been developed to test the passive spring system that allows this new energy storage and delivery method.

Knee behavior can be subdivided in two parts, the weight acceptance phase, characterized by a high joint stiffness and high torque, and the flexion phase, where there

is a high knee flexion of about 60° and a low torque to prevent the leg from extension during swing phase. These knee behaviors can be roughly approximated by using two springs placed between the lower leg and the upper leg. We have named these springs the WA spring, which has a high stiffness, and BL spring, which has a low stiffness. The torque-angle characteristics of these two springs and how they compare to the target knee torque is shown in Figure 7. A schematic of the knee springs can be found in Figure 8, showing the relative positions of the springs to the knee joint center. The realized knee design can be found in Figure 12.

2.2.1. Weight Acceptance System

The WA spring must only be active during only a fraction of the gait cycle directly following the heel strike (see Figure 17 for details about the timing). To insert and remove the effect of the spring on the knee joint torque, a locking mechanism has been developed. This lock allows the knee to perform either large knee flexion at low torque when unlocked or small knee flexion at high torque when locked. The locking of the knee needs to be light and low power if harvesting energy from the knee is to be energetically interesting and the locking mechanism should allow the knee to lock at any angle, effectively determining the rest position of the WA spring. A ratchet and pawl system can satisfy both of these requirements, if implemented correctly [33]. Ideally at full extension the spring and the WA linkage are in a near singular position, meaning the force applied by the spring is directed through the rotation center of the linkage. The WA spring is then locked in place using the ratchet and pawl, and because of the kinematic position of the linkage, a relatively low tension is required in the cable to hold the spring in place. When the pawl is locked, the knee is free to extend because the ratchet locks in only one direction. This allows the locking mechanism to automatically follow the knee during extension, but immediately inhibits flexion of the knee. The spring loaded ratchet and pawl mechanism is then unlocked so the WA linkage can rotate out of the way and the knee can quickly flex to provide sufficient ground clearance for the swing phase.

The actual torque of the WA system is dependent on the state of the locking mechanism, meaning locked or unlocked and the rest position of the WA spring, as well as

the angle of the knee and the geometry of the WA spring at that specific lock state. Although this is a non-linear function, during normal walking the behavior of the spring is relatively linear in the torque-angle space, as illustrated in Figure 7.

2.2.2. Baseline Spring System

The Baseline spring (K_{BL}) is fixed in the system providing a flexion torque as a function of the knee angle. There is no locking mechanism of the baseline spring, nor is there a method of changing the rest position of the spring. The flexion torque provided by the BL spring ranges from approximately -20Nm at full extension to no torque past 65 degrees of knee flexion. Note that this spring resists knee extension, which is contrary to most conventional knees, in order to capture energy from the end of swing phase when the knee generally provides a braking torque to prevent knee overextension.

The torque of the BL spring is a non-linear function of the knee angle, the behavior of which was chosen to track the target knee torque by choosing the mounting points of the spring through simulation. The resultant torque is shown in Figure 7.

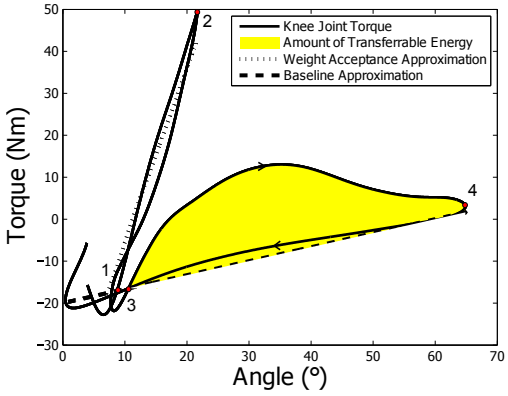

Figure 7: Approximation of the Knee Torques using two springs. The WA phase (between points 1-2-3) is mimicked by the WA spring, while pushoff and swing phases (points 3-4-1) are handled by a combination of the BL spring (shown as dotted line) and the ET system, which provides a positive (extension) joint moment during early pushoff.

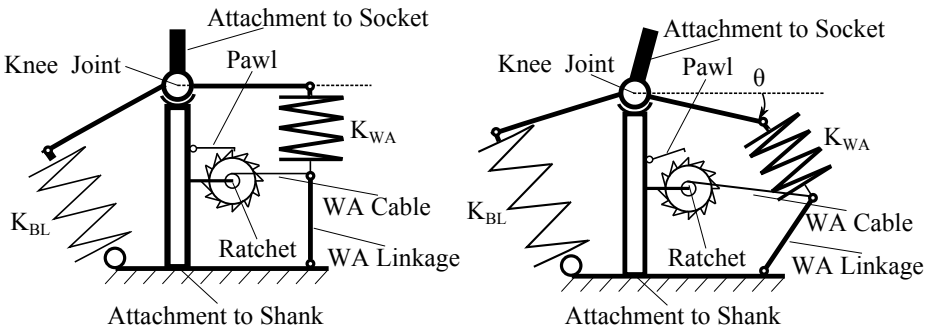

(a) Locked at Full Knee Extension (Straight Leg) (b) Unlocked Knee Bent

Figure 8: Schematic of the Knee Spring Behavior. When locked the WA Linkage and spring are in a near-singular position, allowing the tension in the WA cable to remain low. The lock is only active in the flexion direction, in extension a spring loaded ratchet pulls up slack in the WA cable.

2.2.3. Energy Transfer

The WA and BL springs of the knee joint are not sufficient to completely track the desired torque trajectory. Between the end of the WA and the point of maximum flexion, a torque is needed around the knee joint to prevent the knee joint from collapsing during the pushoff phase (between points 3 and 4 in Figure 7). At this point, the ET locking mechanism directly connects the knee and the ankle through a cable. This energy transfer mechanism provides the necessary knee extension torque, producing negative work directly on the knee joint, and simultaneously transfers stored energy from the baseline spring to the ankle where it can be used for pushoff. The torque provided by the ET system is a mixture of both the knee and ankle behavior, determined around the knee by the force and the effective moment arm of the ET cable. The energy from the knee is then provided at the ankle, where the ankle torque due to the ET is a product of the moment arm of the ankle and the force in the cable.

Simulation of the ET phase consists of calculating the distance between the knee and the ankle moment arms and modeling the cable as a stiff spring to avoid overconstraining the system. Then the knee torque can be calculated as the summation of the torques of the BL spring and the ET mechanism, which must equal the Winter target torque, solving this for the tension in the cable. Then the tension of the cable and the

ankle moment arm determines the torque applied to the ankle, which is equal to the reduction of torque of the ankle actuator.

During normal walking of an able-bodied person, a knee joint primarily dissipates energy [31] providing an opportunity to harvest this energy for use during a different part of the gait cycle. There are two times during the gait cycle which present the possibility to collect and deliver energy to the ankle. These times are at the end of swing phase and during late pushoff, the combined energy of these two periods is displayed in the yellow shaded section of Figure 7.

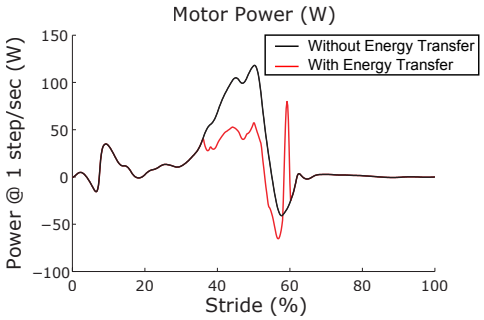

Figure 9: Motor power required to match the average ankle torque with (red line) and without (black line) energy transfer from the knee. The negative work done by the knee is brought to the ankle using a cable system. The additional torque provided by the knee reduces the torque required at the ankle joint, reducing the overall power requirement at the ankle.

At the end of swing phase, the ankle does not need power, and therefore the energy harvested during this period of the gait cycle must be stored in the baseline spring at the front of the knee. Then the coupling mechanism is locked during stance and pushoff, providing a direct kinematic constraint between the knee and the ankle. This kinematic constraint allows the torque generated by the baseline spring and the ankle-knee kinematic constraint to effectively transfer energy to the ankle at the end of pushoff, creating the torque-angle relationship from points 3 back to 1 in Figure 7. Transferred energy is delivered with a slightly delayed ankle pushoff when compared to normal gait in order to transfer maximum energy, meaning the ankle angle slightly trails what it would if it were a normal gait cycle. Because this energy is now provided at the moment where the ankle torque is the highest, there is a large reduction in torque that

the ankle actuator must provide.

In Figure 9, the reduction in motor power due to the energy transfer mechanism required to match the average ankle torque is illustrated. The power peaks are lower and there is an overall drop in energy usage of about 30% (7J reduction compared to a total consumption of 22J per step) as well as a 25% drop in peak power. Figure 10 shows the knee mechanism as it is attached to the knee joint. A single toothed ratchet is centered on the joint axis and is locked in place by the ET pawl. This locks the ratchet relative to the top of the knee joint. The ratchet is also attached to a cable that is connected to the rear of the foot. As the ratchet rotates, it pulls the cable, plantarflexing the foot. Another feature of the design is that once the knee flexes past a certain point, the cable automatically unlocks because the attachment of the cable travels through the knee joint center and the cable tension pulls the ratchet in the opposite direction, effectively unlocking it. The angle at which this happens can be set independently, as can the rest position of the ankle. When unlocked, the ratchet is returned to the neutral position by a small return spring but is free to move with respect to the top of the knee and so as the knee flexes, the cable is not pulled.

3. Materials and Methods

The completed prosthesis with motor drivers, shoe, insole, and cosmetic cover weighed 5.2kg, which is comparable to a normal human leg, but considerably more than most commercial passive prostheses. The system is comparable in weight to the state of the art active prostheses, such as the Ossur Power Knee (3.19 kg, with batteries) paired with the BiOM T2 (2.3 kg, with batteries). It should be noted that the Alpha-Prosthesis has not been optimized for weight, and in fact can not largely deviate from the mass and inertia of a normal human leg for the dynamics to work as simulated. It is primarily a test bed for the new actuators and passive spring principles of the knee.

3.1. Ankle

The new redesigned actuator solves many of the problems with previous MACCEPA designs, such as removing cable systems and using compact compression springs.

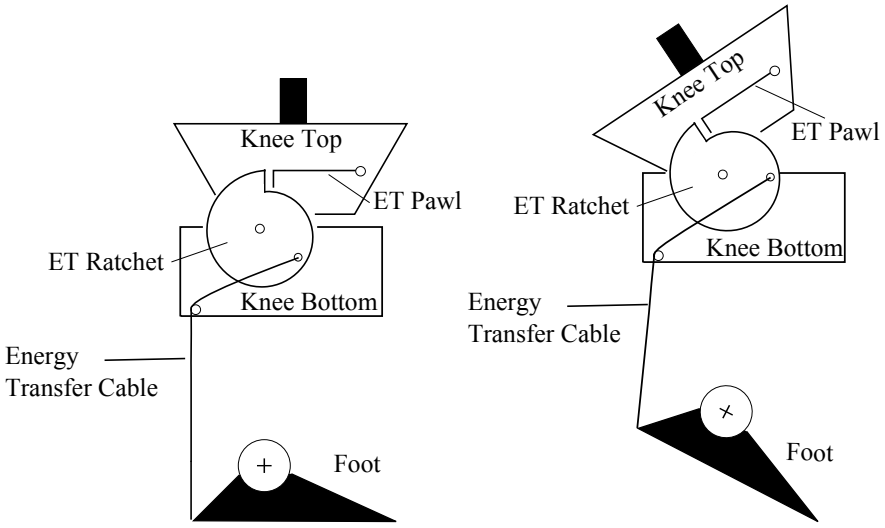

(a) Locked ET mechanism at full knee extension.

(b) Locked ET mechanism while knee is flexed, kinematically linking the knee and ankle.

Figure 10: Schematic of the Knee Energy Transfer Mechanism. As the locked mechanism flexes, the cable directly couples the kinematics of the knee and the ankle. When the ET ratchet is unlocked, the knee and ankle move independently.

The system also is capable of providing 130 Nm torque at the ankle, a requirement to provide full normal joint torque and higher than previous designs by a factor of two. The actuator also had firm size constraints requiring us to fit inside a size 42(EU) shoe because of the insole sensors [34] that were to be used with this prototype.

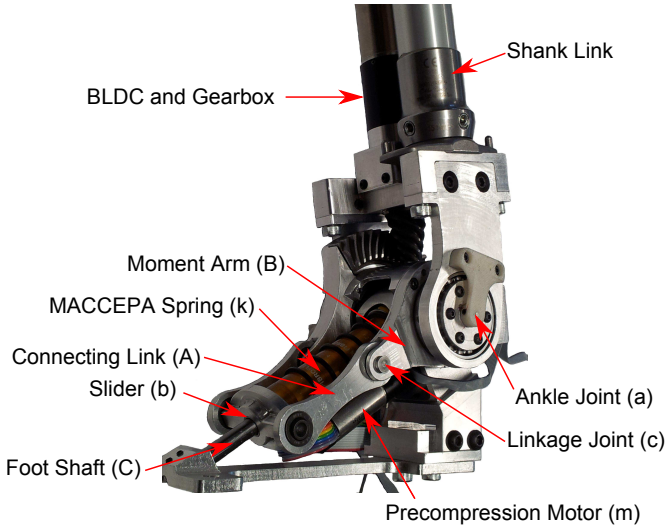

Figure 11: Implementation of the MACCEPA actuator. Compare to Figure 1.

Figure 11 shows all of the physical components of the ankle that correspond to the schematic in Figure 1. There is a plastic plate that is used to provide toe flexion and a rubber cosmetic cover that fit over the mechanism and allow it to fit snug within a shoe. The cosmetic cover also provides a smooth surface to interface with the insoles used for center of pressure measurements.

The main motor for the ankle actuator is a Maxon RE30 ($60W$) and utilizes a large $10:1$ ratio hypoid gear as a final drive stage and an initial gear stage of an $86:1$ planetary gear system. This motor was not the original motor chosen for the system, as was shown in the ankle motor simulations, but was ultimately chosen due to time constraints for the integration of the system in Italy. Although the MACCEPA architecture lowers the peak power required by the motor, the torque of the system remains the same, meaning the gear drive system needs to be able to handle the full torque of the output.

The pretension mechanism is housed under the MACCEPA spring, comprised of a Maxon ECMax 16, 8W motor with a 1621 : 1 ratio planetary gearbox connected to a custom 1.2 : 1 final stage. This final drive contains an ACME nut with a 3mm lead which compresses the main spring against the slider. This system is represented as m in Figure 1. The pretension motor is not powerful enough to compress the spring under actuation or drive the load fast enough to change precompression during the gait cycle. Instead it is used over many gait cycles to tune the gait as necessary, particularly to change the required velocity characteristics of the moment arm.

3.2. Knee

Figure 12 shows the rear of the physical realization of the schematics in Figures 8 and 10. Here we can see both of the ratchet mechanisms on the inner sides of the knee structure, as well as the two springs.

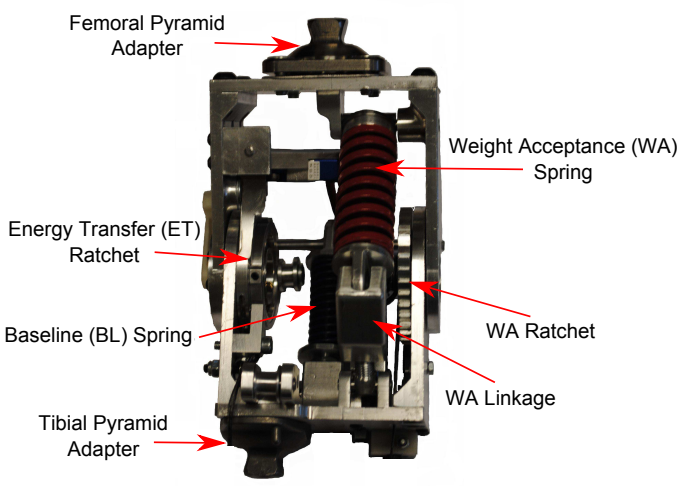

Figure 12: Rear view of Knee Displaying the Locking Mechanisms and Springs. The Baseline Spring (blue) is on the front of the knee and is seen to the left of the Weight Acceptance Spring (red).

3.3. Sensors and Control System

The control system runs on a real-time controller, a cRIO 9082 (National Instruments, Austin, Texas, US), endowed with a 1.33 GHz dual-core processor running

a NI real-time operating system and a Field Programmable Gate Array (FPGA) processor Spartan-6 LX150. This system is not only responsible for the prosthesis, but also for the CYBERLEGs exoskeleton and sensing arrays. The main ankle motor is controlled by means of a commercial servo driver EPOS2 70/10 (Maxon Motor AG, Sachseln, Switzerland), while the pretension system is driven by a Maxon EPOS2 24/2. A closed-loop PID controller is used to control the MACCEPA moment arm position, a schematic of the control system can be found in Figure 5. Control of the reference signal for the MACCEPA as well as for the locking-unlocking mechanisms is based on the estimates of the vertical ground reaction force and coordinates of the center of pressure gathered by means of two 64-channel pressure-sensitive insoles embedded into the sport shoes worn by the amputee [34] (see section 4.2 for details about how this was used in the trials). This initial finite state machine control system is intended to only provide basic capabilities for testing and validation purposes and will be later replaced by a novel hybrid control system based on motor primitives and feedback reflexes [35, 36].

4. Experiments

First a characterization of the ankle actuator was performed to investigate the new MACCEPA behavior under a cyclical torque as seen during walking. Then the prosthesis was worn by a number of amputee subjects to tune the initial state machine and evaluate the behavior of the device in actual use.

4.1. Ankle Bench Tests

The ankle actuator was fixed to a test apparatus and a torsional load cell was attached coincident with the ankle axis. The load cell was then fixed to the apparatus, locking the ankle joint angle. A commanded torque signal at 70% of the amplitude and at 2 seconds/stride was created from the Winter torque data, based on expected performance of the subjects. The desired torque signal was sent to the controller, seen in Figure 5, and the output torque of the actuator was measured by the external load cell at 1 kHz.

The force on the external torque transducer was compared with the calculated torque from the MACCEPA load cell mounted in the actuator and it was found that the readings matched within a few percent, lending confidence to the calculated values from the internal load cell measurements.

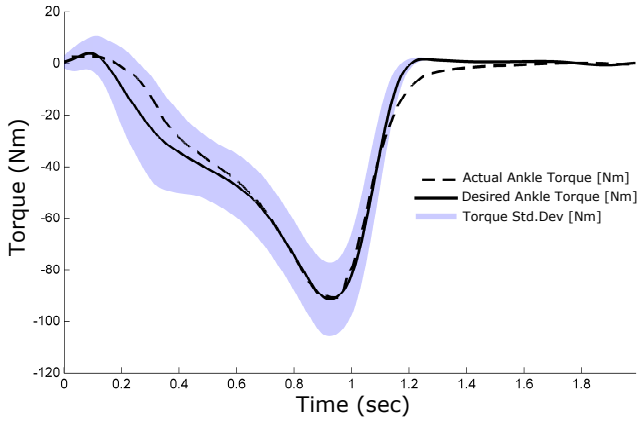

Figure 13: Desired and actual output torque of the ankle actuator. The target is set to 70% of the total joint torque at 2 sec/stride. This test was using the Maxon EC-4pole 30 with an 86:1 gearbox.

The actuator was able to track the torque command reasonably well, staying within the standard deviation of the measured torque data from Winter during most of the stride. There is some tracking error particularly after the pushoff phase as the moment arm must swing from fully plantarflexed to the dorsiflexion side of the foot, as can be seen in Figure 13.

4.2. Walking Tests

Initial trials to fine tune the mechanics of the prosthesis were performed using a bent knee cast on healthy individuals at Scuola Superiore Sant'Anna, Pontedera, Italy. Later the device was transferred to be tested on three amputee subjects at the Fondazione Don Carlo Gnocchi in Florence, Italy. These subjects walked along a 10m long catwalk, as preferred by the patients. Figure 14 shows a typical stride of a subject down the catwalk. The prosthesis was tethered to the control system which was housed on a cart traveling beside the patient.

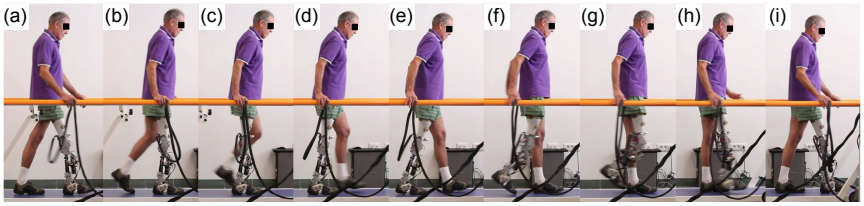

Figure 14: Gait phases of an amputee walking. From left to right: a) Heel strike of the prosthesis. b) Toe off of the sound limb. c) Early swing of the sound limb. d) Mid stance of prosthetic limb and late swing of the sound limb. e) Heel off of prosthetic limb and heel strike of the sound limb. f) End of double support and toe off of the prosthetic limb. g) Early swing of the prosthetic limb. h) Late swing of prosthetic limb and mid stance of the sound limb. i) Heel strike of prosthetic limb.

Preliminary testing with both intact and amputated limbs has proven successful, with one significant caveat. During these early trials the moment arm position was commanded to half of the full range of torque required by the ankle during normal gait because of problems with bandwidth limitations of the actuator. The low bandwidth was due to changing the motor to a much smaller 60W Maxon RE30 motor at the test site due to limitations with the initial motor drivers sourced for the project. The motor/gearbox combination used in these tests were much slower than the initial design suggested, in fact they are approximately four times slower than the bench tested drives, but used so that integration into the larger CYBERLEGs system could be expedited. The pretension of the system was chosen by pre-selecting a value based on the behavior during test walks, in most cases around 7mm (900N) of pretension was used.

Because the actuator was slow, it could not reach the full range necessary to meet the mean trajectory from the Winter Data in the timeframe of one step, and required careful timing of the state machine to achieve suitable ground clearance. This can be seen in Figure 15, as the toe extension has been omitted at the end of pushoff in order to move the toe in position for the swing phase. Bandwidth tests showed the cutoff frequency of the actuator at 60 Nm to be around 0.43 Hz, and although in simulation this reaches within the standard deviation of the normal gait cycle, it causes noticeable problems such as low toe clearance due to the slow dorsiflexion of the ankle after pushoff. Also the excessive dorsiflexion at the beginning of the step is a result of the slow moment arm movement, which can also been seen in the simulation (Figure 6).

The highly limited moment arm velocity was by far the limiting factor in performance of the prosthesis, but even with low torque and resulting deviation of the kinematics, we were able to achieve adequate ground clearance in the swing phase during the trials and show a positive injection of energy at the ankle joint. With a small change to the motor of the system, as in the simulations the velocity profile should be greatly improved and we expect velocity related problems, such as toe clearance during swing, to be greatly reduced.

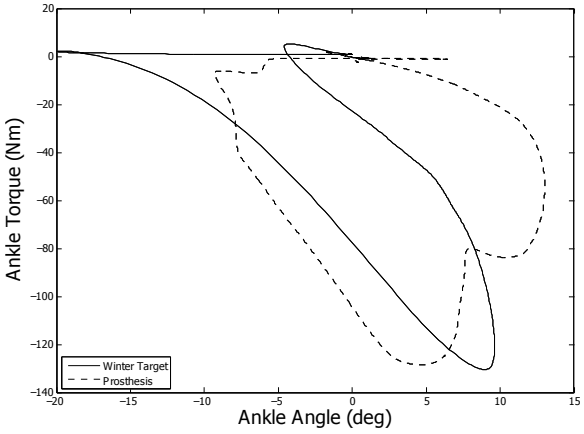

Figure 15: Ankle Torque-Angle Characteristics during first walking trials. The area of the loop is in the clockwise direction, with a negative torque, indicating energy injection into the system.

Initial datasets were created using a finite state machine using the center of pressure location of the insole sensors to trigger gait state transitions. A sample dataset from an amputee subject can be found in Figure 16. Here we can see the gait state determined by the insoles, which in turn drive the desired MACCEPA moment arm position. The gait is broken into 4 sections, the Swing Phase (SW), Early Stance (ES), Mid Stance (MS), and Late Stance (LS). Swing Phase is determined by the single support phase of the sound leg, Early Stance is defined as the double support phase after heel strike of the prosthesis, Mid Stance is the single support phase of the prosthesis, and Late Stance is the double support phase after the sound leg heel strike. Other methods were used during the trials to determine the state changes, such as center of pressure thresholds. This technique changed the gait state when the center of pressure of the

stance foot passed a certain point on the sole. As the state machine was only used for validation purposes, the exact method of state triggering was not rigorously evaluated. Each of the states held a preset moment arm trajectory (des MA in red in Figure 16), determined by a linear fit to the trajectories found in simulation. These were then modified empirically to achieve suitable ground clearance and pushoff behavior. We also saw good knee flexion during swing and a prolonged stance flex stage, ended by knee extension at the beginning of pushoff.

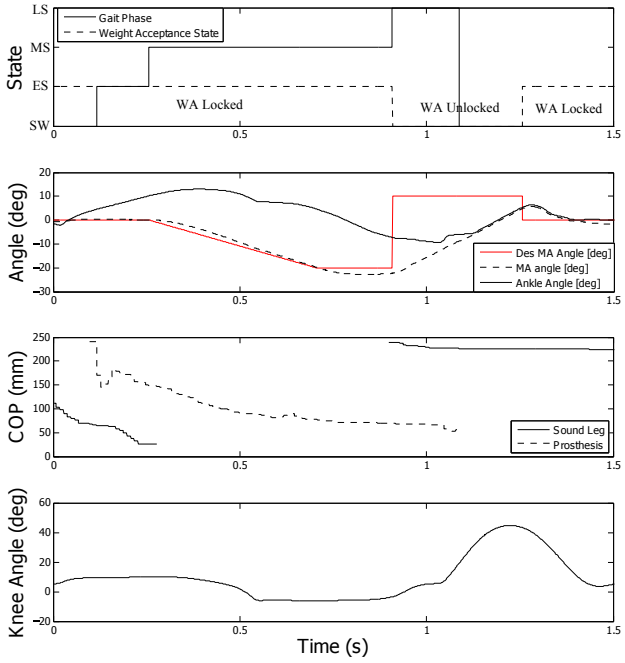

Figure 16: Preliminary datatset from the first prosthesis trials. Use of an early finite state machine with a conservative moment arm position with low torque. The state values are described as the Swing Phase (SW), Early Stance (ES), Mid Stance (MS), and Late Stance (LS). The red moment arm position is the approximation for the desired moment arm position used in the initial state machine trials with the energy transfer system in place.

The baseline spring was also adjusted with a lower spring constant of 5 N/mm to better match the gait speed of the patient. The preferred walking speed of the amputees was considerably slower ($\approx 1.5 sec/stride$ compared to $1 sec/stride$) than the target kinematics, and therefore there was less energy in the swing phase to store in the

baseline spring.

4.3. Walking With Energy Transfer

During these tests, the energy transfer mechanism was installed and the state machine was updated. Whereas before the weight acceptance spring remained locked during the whole single support phase of the amputated leg to make up for the lack of extension torque when the energy transfer system was not being utilized, with the energy transfer mechanism in the system the knee stiffness during this phase is guaranteed. This can be seen in the locking diagram in Figure 17. The WA mechanism was unlocked based on the center of pressure measurement in the insole. When the center of pressure passed a certain threshold, the state machine ended the weight acceptance and locked the energy transfer mechanism. The tests were performed by a transfemoral amputee on the same 10 m long catwalk as used for the previous walking tests. The amputee walked about 4 steps with the prosthesis every run and each run he switched the leg with which he initiated the gait.

The energy transfer cable was connected between the ankle and the knee lever arms and tensioned by rotating the lever arms into their calculated optimal initial positions. For the knee lever arm, the locking position corresponds to an angle of 110° between the upper leg and the lever arm. For the ankle the position of the moment arm is at 120° with respect to the shank. After an initial run the measured data were analyzed and the lever arm positions and cable length were adjusted. This was done again after every five test runs for a total of 20 test runs.

Figure 18 shows the timing of the energy transfer cable force with the ankle torque. As the knee joint bends, the locked cable creates a torque around the ankle, reducing the moment required by the actuator motor at exactly the time when peak torque is required by the actuator. In this figure, the force in the cable corresponds to an ankle torque of approximately $3.6Nm$, which is negligible for energy consumption measurements. The expected force in the cable should be around $650N$ when tuned correctly, resulting in a $20Nm$ reduction in the torque required by the ankle actuator. Reducing the maximum torque the ankle motor has to apply during pushoff can reduce the energy consumption of the prosthesis from $1J$ up to $12J$ per step if the timing is correct between the knee and

the ankle. This could potentially mean a reduction between 6 and 65% in the power required from the motor output. The tuning of this mechanism is extremely critical, and due to the low number of steps during a walking trial, it was difficult to reach a steady state and consistent gait for good power measurements of this system. For better measurements, it would be beneficial to have treadmill trials, but none of the patients felt comfortable enough to use the prosthesis on the treadmill with so little training time.

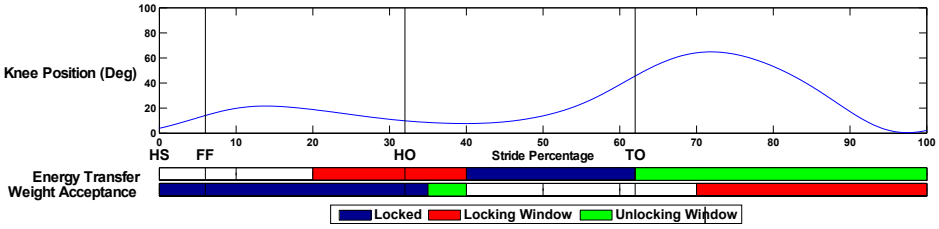

Figure 17: Locking Diagram for the Knee Locks, including the Energy Transfer System. Shows the timing of the locking of the Weight Acceptance spring and the Energy Transfer System, with respect to the desired knee angle and the Heel Strike (HS), Foot Flat (FF), Heel Off (HO), and Toe Off (TO) times of the prosthesis.

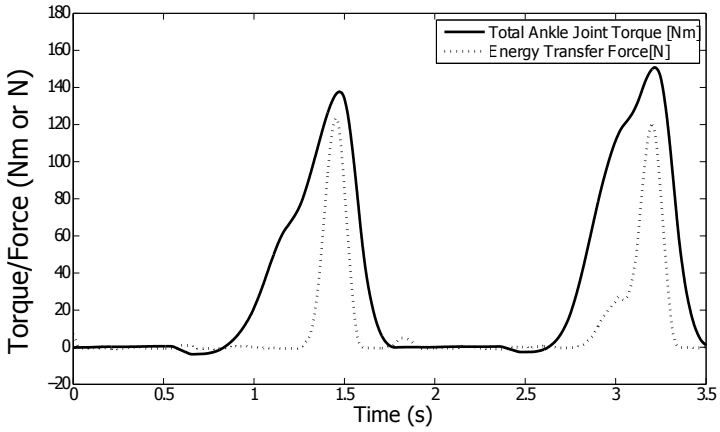

Figure 18: The timing of the Energy Transfer cable force at the peak of pushoff. Although the timing of the force in the ET cable is correct, the absolute torque produced during the trial is low due to tuning of the system. During this trial, the torque amounts to approximately 3.6Nm, which is negligible for energy consumption measurements. The expected force in the cable should be around 650N when tuned correctly.

5. Discussion

5.1. Ankle and Knee

The ankle actuator has performed well throughout the trials, providing energy input to the ankle as planned. It was not expected that the current motor/gearbox combination could track the average Winter ankle kinematics exactly, but it has shown clear injection of energy into the gait cycle.

Changing the pretension of the MACCEPA during the gait cycle has not been properly investigated because the prototype does not allow for this capability. However, it is possible that if we were able to vary the stiffness properties of the spring using the pretension mechanism during the gait cycle, the total energy consumption of the system may be reduced. There is also the potential for the pretension motor to work against the main motor, causing a dramatic increase in energy consumption. Although it would be possible to optimize the tuning for both motors using the results from the simulations, it is hard to predict the exact behavior of the prosthesis when being worn by an amputee. In addition, Winter's biological data are given as averages from a number of subjects, and inter-subject variation must be accounted for through individual tuning. Given the complexity of the rest of the system, it is better to only actuate the pretension mechanism between trials, to change the overall behavior of the actuator for these initial trials.

5.2. Transferred energy

As discussed before, according to the preferences of the test subjects, a lighter baseline spring and lower walking speed was used in the trials than what was calculated in the simulations. As a consequence, less energy can be stored during the end of the swing phase, and less energy can be transferred to the ankle joint. In simulations a stiff spring was considered in the energy transfer mechanism as both the knee and the ankle joint angles have been used as an input. For the experiments the elasticity of the mechanism and cable were expected to be high enough to approximate this high stiffness. The downside of this high stiffness is that the positioning of the moment arms has to be very precise, as small variations in the length of the cable have a big impact on the energy transfer.

Tuning the mechanism for an optimized energy transfer is something that could not be done easily with the current design. The next design, currently in development, will allow changing the cable length by means of a motor and separate from the moment arm angles, which will greatly increase the tuneability. Other factors that could increase the transferred energy are longer runways or executing experiments on a treadmill, which would allow the amputee to reach a steady state allowing for consistent measurements. The active prosthesis is a device that differs from the passive devices the test subjects are used to, so more training is necessary to obtain good results.

5.3. Achievements

The prosthesis has proven that using a active ankle with a primarily passive knee and knee to ankle energy transfer system can work. The ankle has shown a good power injection during the gait cycle. The knee has shown a good knee flexion during swing allowing suitable toe clearance, while providing the required stiffness during stance phase. The energy transfer system shows that a knee to ankle transfer system can work, with the timing of the force between the knee and the ankle correctly applied during the pushoff phase.

6. Conclusions

The CYBERLEGs Alpha-Prosthesis was designed to test the behaviors of three systems: a new compliant ankle actuator, a new passive knee utilizing springs to store braking energy from the knee, and an energy transfer mechanism to deliver the stored energy of the knee to the ankle. These devices have been successfully used by amputees in a limited three subject trial. This design philosophy is very different from current passive prostheses, which generally utilize dampers in the knee to dissipate the braking energy and keep knee and ankle prostheses separate from one another. The results are promising, showing that there is an injection of energy at the ankle, assisting the pushoff, the passive knee is capable of producing reasonable knee kinematics with a nice natural swing phase, and the energy transfer mechanism is capable of producing a torque on the ankle form the knee at the correct time during the gait cycle.

The current control system incorporates the use of pressure-sensitive foot insoles to determine the state of the gait cycle on-line and control the knee and ankle modules, as well as their mechanical coupling. Recorded data and feedback from both healthy and amputated subjects have proven successful performance and encourage a more extensive experimental characterization, including the effect of actuator pretension, on the energetics of the gait cycle and the effects of the energy transfer mechanism. The device has proved to be a valuable testbed for multiple control schemes translating the user motion intentions into motor commands to incorporate the prosthesis within the larger CYBERLEGs framework.

Future work includes expanding upon the passive mechanism of this design with actuation, and a prosthesis is currently in development. This will allow sit to stand and stair climbing operations in addition to efficient walking. This new system will also allow easier tuning and individualization of the ET mechanism and a more reliable WA system.

7. Acknowledgments

This work has been funded by the European Commission 7th Framework Program as part of the CYBERLEGs project, grant no. 287894. The second author is funded by a Ph.D. grant of the Agency for Innovation by Science and Technology in Flanders (IWT). The authors would also like to thank Marnix De Boom and Marc Luypaert for their work building the Alpha-Prosthesis.

References

[1] T. R. Dillingham, L. E. Pezzin, E. J. MacKenzie, Limb amputation and limb deficiency: epidemiology and recent trends in the United States., Southern Medical Journal 95(8) (2002) 875–883.

[2] K. Ziegler-Graham, E. J. MacKenzie, P. L. Ephraim, T. G. Travison, R. Brookmeyer, Estimating the prevalence of limb loss in the United States: 2005 to 2050., Archives of physical medicine and rehabilitation 89 (3) (2008) 422–9.

doi:10.1016/j.apmr.2007.11.005.
URL http://www.ncbi.nlm.nih.gov/pubmed/18295618

[3] R. L. Waters, J. Perry, D. Antonelli, H. Hislop, Energy cost of walking of amputees : the influence of level of amputation The Influence of Walking of Level of Amputees : of Amputation, J Bone Joint Surg Am. 58 (1976) 42–46.

[4] K. R. Kaufman, J. A. Levine, R. H. Brey, S. K. Mccrady, D. J. Padgett, M. J. Joyner, Energy Expenditure and Activity of Transfemoral Amputees Using Mechanical and Microprocessor-Controlled Prosthetic Knees, Archives of Physical Medicine and Rehabilitation 89 (July) (2008) 1380–1385. doi:10.1016/j.apmr.2007.11.053.

[5] J. J. Genin, G. J. Bastien, B. Franck, C. Detrembleur, P. A. Williems, Effect of speed on the energy cost of walking in unilateral traumatic lower limb amputees, Eur J Appl Physiol 103 (2008) 655–663. doi:10.1007/s00421-008-0764-0.

[6] A. B. Sawers, B. J. Hafner, Outcomes associated with the use of microprocessor-controlled prosthetic knees among individuals with unilateral transfemoral limb loss: a systematic review., Journal of rehabilitation research and development 50 (3) (2013) 273–314.
URL http://www.ncbi.nlm.nih.gov/pubmed/23881757

[7] J. K. Hitt, R. Bellman, M. Holgate, T. G. Sugar, K. W. Hollander, The SPARKy (Spring Ankle with Regenerative Kinetics) project: Design and analysis of a robotic transtibial prosthesis with regenerative kinetics, in: ASME International Design Engineering Technical Conferences & Computers and Information in Engineering Conference IDETC/CIE 2007, Las Vegas, Nevada, USA, 2007, pp. 1587–1596.

[8] S. Au, M. Berniker, H. Herr, Powered ankle-foot prosthesis to assist level-ground and stair-descent gaits., Neural Networks 21 (4) (2008) 654–66. doi:10.1016/j.neunet.2008.03.006.
URL http://www.ncbi.nlm.nih.gov/pubmed/18499394

[9] Ossur, www.ossur.com (2013).

[10] P. Cherelle, V. Grosu, A. Matthys, B. Vanderborght, D. Lefeber, Design and Validation of the Ankle Mimicking Prosthetic (AMP-) Foot 2.0, Neural Systems and Rehabilitation Engineering, IEEE Transactions on PP (99) (2013) 1. doi:10.1109/TNSRE.2013.2282416.

[11] R. D. Bellman, M. a. Holgate, T. G. Sugar, SPARKy 3: Design of an active robotic ankle prosthesis with two actuated degrees of freedom using regenerative kinetics, IEEE RAS & EMBS International Conference on Biomedical Robotics and Biomechatronics (2008) 511–516doi:10.1109/BIOROB.2008.4762887.
URL http://ieeexplore.ieee.org/lpdocs/epic03/wrapper.htm?arnumber=4762887

[12] J. Zhu, Q. Wang, L. Wang, On the Design of a Powered Transtibial Prosthesis with Stiffness Adaptable Ankle and Toe Joints, Industrial Electronics, IEEE Transactions on PP (99) (2013) 1. doi:10.1109/TIE.2013.2293691.

[13] A. H. Shultz, J. E. Mitchell, D. Truex, B. E. Lawson, M. Goldfarb, Preliminary Evaluation of a Walking Controller for a Powered Ankle Prosthesis, IEEE International Conference on Robotics and Automation (2013) 4823–4828.

[14] E. C. M. Villalpando, J. Weber, G. Elliott, H. Herr, A. State, Design of an Agonist-Antagonist Active Knee Prosthesis, IEEE/RAS-EMBS International Conference on Biomedical Robotics and Biomechatronics (2008) 529–534.

[15] F. Sup, H. A. Varol, J. Mitchell, T. J. Withrow, M. Goldfarb, Preliminary Evaluations of a Self-Contained Anthropomorphic Transfemoral Prosthesis., IEEE/ASME Transactions on Mechatronics 14 (6) (2009) 667–676. doi:10.1109/TMECH.2009.2032688.
URL http://www.pubmedcentral.nih.gov/articlerender.fcgi?artid=2801882&tool=pmcentrez&rendertype=abstract

[16] K. W. Hollander, R. Ilg, T. G. Sugar, D. Herring, An efficient robotic tendon for gait assistance., Journal of Biomechanical Engineering 128 (5) (2006) 788–91.

doi:10.1115/1.2264391.
URL http://www.ncbi.nlm.nih.gov/pubmed/16995768

[17] S. Au, H. Herr, Powered ankle-foot prosthesis, IEEE Robotics & Automation Magazine 15 (3) (2008) 52–59. doi:10.1109/MRA.2008.927697.
URL http://ieeexplore.ieee.org/lpdocs/epic03/wrapper.htm?arnumber=4624583

[18] B. Vanderborght, A. Albu-Schaeffer, A. Bicchi, E. Burdet, D. Caldwell, R. Carloni, M. Catalano, O. Eiberger, W. Friedl, G. Ganesh, M. Garabini, M. Grebenstein, G. Grioli, S. Haddadin, H. Hoppner, A. Jafari, M. Laffranchi, D. Lefeber, F. Petit, S. Stramigioli, N. Tsagarakis, M. V. Damme, R. V. Ham, L. Visser, S. Wolf, Variable impedance actuators: A review, Robotics and Autonomous Systems 61 (12) (2013) 1601 – 1614. doi:http://dx.doi.org/10.1016/j.robot.2013.06.009.
URL http://www.sciencedirect.com/science/article/pii/S0921889013001188

[19] SpringActive, ODYSSEY, http://www.springactive.com/.

[20] IWalk, BiOM, http://www.iwalk.com/.

[21] H. M. Herr, A. M. Grabowski, Bionic ankle-foot prosthesis normalizes walking gait for persons with leg amputation, Proc. Roy. Soc. Lon. B 279 (2012) 457–464.

[22] E. J. Rouse, L. M. Mooney, E. C. Martinez-Villalpando, H. M. Herr, Clutchable series-elastic actuator: Design of a robotic knee prosthesis for minimum energy consumption., IEEE International Conference on Rehabilitation Robotics 2013 (1122374) (2013) 1–6. doi:10.1109/ICORR.2013.6650383.
URL http://www.ncbi.nlm.nih.gov/pubmed/24187202

[23] A. O. Kapti, M. S. Yucenur, Design and control of an active artificial knee joint, Mechanism and Machine Theory 41 (12) (2006) 1477–1485. doi:10.1016/j.mechmachtheory.2006.01.017.

URL http://linkinghub.elsevier.com/retrieve/pii/S0094114X06000243

[24] Y. Geng, X. Xu, L. Chen, P. Yang, Design and analysis of active transfemoral prosthesis, IECON Conference on IEEE Industrial Electronics Society (2010) 1495–1499doi:10.1109/IECON.2010.5675461.
URL http://ieeexplore.ieee.org/lpdocs/epic03/wrapper.htm?arnumber=5675461

[25] A. Staros, E. F. Murphy, Properties of fluid flow applied to above-knee prostheses, Bulletin of Prosthetics Research Spring (1964) 40–65.

[26] A. Matthys, P. Cherelle, M. Van Damme, B. Vanderborght, D. Lefeber, Concept and design of the HEKTA (Harvest Energy from the Knee and Transfer it to the Ankle) transfemoral prosthesis, in: IEEE International Conference on Biomedical Robotics and Biomechatronics, 2012, pp. 550 – 555. doi:10.1109/BioRob.2012.6290833.

[27] R. Unal, S. M. Behrens, R. Carloni, E. E. G. Hekman, S. Stramigioli, H. F. J. M. Koopman, Prototype Design and Realization of an Innovative Energy Efficient Transfemoral Prosthesis, in: Proceedings of the 2010 3rd IEE RAS & EMBS International Conference on Biomedical Robotics and Biomechatrionics, 2010, pp. 191–196.

[28] R. Van Ham, B. Vanderborght, M. van Damme, B. Verrelst, D. Lefeber, MACCEPA, the mechanically adjustable compliance and controllable equilibrium position actuator: Design and implementation in a biped robot, Robotics and Autonomous Systems 55 (10) (2007) 761–768.

[29] J. Pratt, B. Krupp, C. Morse, Series elastic actuators for high fidelity force control (2002). doi:10.1108/01439910210425522.

[30] OttoBock, www.ottobock.com (2013).

[31] Winter, D.A., Biomechanics and Motor Control of Human Movement, John Wiley and Sons, United States of America, 2005.

[32] P. Beyl, M. Van Damme, R. Van Ham, B. Vanderborght, D. Lefeber, Design and control of a lower limb exoskeleton for robot-assisted gait training, Applied Bionics and Biomechanics 6:2 (2009) 229–243. doi:10.1080/11762320902784393.

[33] J. Geeroms, L. Flynn, R. Jimenez-Fabian, B. Vanderborght, D. Lefeber, Design, development and testing of a lightweight and compact locking mechanism for a passive knee prosthesis, IEEE International Conference on Biomedical Robotics and Biomechatronics. (2014).

[34] M. Donati, et. al., A Flexible Sensor Technology for the Distributed Measurement of Interaction Pressure, Sensors 13 (1) (2013) 1021–1045.

[35] R. Ronsse, N. Vitiello, T. Lenzi, J. van den Kieboom, M. Carrozza, A. Ijspeert, Humanrobot synchrony: Flexible assistance using adaptive oscillators, IEEE Transactions on Biomedical Engineering 58 (4) (2011) 1001–1012. doi:10.1109/TBME.2010.2089629.

[36] R. Ronsse, T. Lenzi, N. Vitiello, B. Koopman, E. Asseldonk, S. Rossi, J. Kieboom, H. Kooij, M. Carrozza, A. Ijspeert, Oscillator-based assistance of cyclical movements: model-based and model-free approaches, Medical & Biological Engineering & Computing 49 (10) (2011) 1173–1185. doi:10.1007/s11517-011-0816-1.
URL http://dx.doi.org/10.1007/s11517-011-0816-1

8. Appendix

To clarify the derivations of Equations 2 and 3, we add the following appendix.

The actuator analysis is conducted under static conditions, with the configuration found in Figure 19.

The actuator has 3 links, where link C is aligned with the x-axis. C also varies in length as the slider containing point b moves along the x-axis. The actuator is constrained by a pin joint at point a and a rolling contact at point b, which constrains the slider in the positive and negative vertical directions.

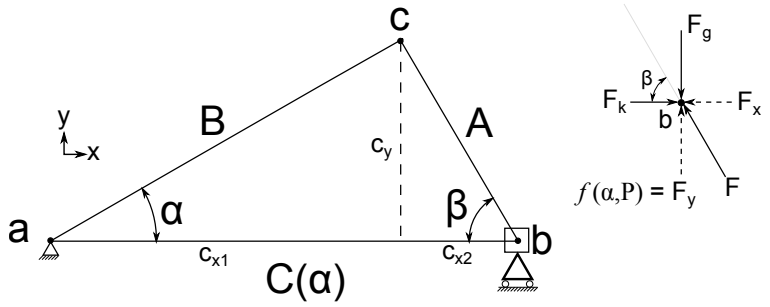

Figure 19: The actuator configuration in the constrained static condition. The force balance on the sliding point b is shown to the right.

By examining the force balance at point b, we can see the force due to the compressed MACCEPA spring is defined as F_k, and the force due to the actuator linkage on point b is F. The direction of this force is at an angle β with respect to the horizontal and varies with the MACCEPA moment arm angle α. The components of F along the x and y axes are called F_x and F_y, respectively. F_g is the vertical constraint force due to the contact of the slider. F_y is the vertical component of the actuator force, and is the same force from Equation 3, $f(\alpha,P)$.

By the force balance for the static system, it can be shown that

$$F_k = -F_x \tag{6}$$

and so

$$\tan(\beta) = \frac{F_y}{-F_k} \tag{7}$$

Using the law of cosines to solve for $C(\alpha)$ yields

$$C(\alpha) = B\cos\alpha + A\left[1 - \left(\frac{B}{A}\sin\alpha\right)^2\right]^{1/2} \tag{8}$$

the same result found in Equation 2. This segment can be broken into two components, C_{x1} and C_{x2} shown in Figure 19, as

$$C_{x1} = B\cos\alpha \tag{9}$$

$$C_{x2} = A\left[1 - \left(\frac{B}{A}\sin\alpha\right)^2\right]^{1/2} \tag{10}$$

By inspection,

$$C_y = B\sin\alpha \tag{11}$$

and therefore β can be defined in terms of α as

$$\tan(\beta) = \frac{C_y}{-C_{x2}} \tag{12}$$

Combining Equations 7 and 12, we see that

$$F_y = \frac{F_k * C_y}{C_{x2}} \tag{13}$$

and by substitution,

$$f(\alpha, P) = \frac{F_k * B\sin\alpha}{A\left[1 - \left(\frac{B}{A}\sin\alpha\right)^2\right]^{1/2}} \tag{14}$$

The spring force is defined as the spring constant k times the displacement of the spring, which can be determined from Figure 1 as

$$F_k = k(P + A + B - C(\alpha)) \tag{15}$$

A final substitution shows that

$$f(\alpha, P) = \frac{kB(P + A + B - C(\alpha))\sin\alpha}{A\left[1 - \left(\frac{B}{A}\sin\alpha\right)^2\right]^{1/2}} \tag{16}$$

as defined in Equation 3.

9. Vitae

Include in the manuscript a short (maximum 100 words) biography of each author, along with a passport-type photograph accompanying the other figures.

Louis Flynn received his MS in Mechanical Engineering from Michigan State University in 2009. He is currently a PhD student at the Vrije Universiteit Brussel developing actuated prostheses and exoskeletons.

Joost Geeroms obtained his Master's degree from the Vrije Universiteit Brussel in 2011. He is currently a Ph.D. student and funded by a Ph.D. grant of the Agency for Innovation by Science and Technology Flanders (IWT). His research is centered on actuated prosthetics.

Rene Jimenez-Fabian received his Doctoral degree in engineering from Universidad Nacional Autnoma de Mxico in 2006. His work focuses on the application of con-

trol and parameter identification techniques to the development of electromechanical systems. He is currently working on the CYBERLEGs project addressing some issues related to the mechanical design, instrumentation, and control of an active lower-limb prosthesis.

Prof. dr. ir. Bram Vanderborght received his PhD in 2007. The focus of his research was the use of adaptable compliance of pneumatic artificial muscles in the dynamically balanced biped Lucy. In 2006 he performed research on the humanoids robot HRP-2 in AIST, Tsukuba (Japan). From October 2007-April 2010 he worked as post-doc researcher at IIT (Italy). Since October 2009, he is appointed as professor at the VUB. He is member of the Young Academy of the Royal Flemish Academy of Belgium for Science and the Arts. In 2013 he received an ERC Starting Grant. His research interests include cognitive and physical human robot interaction with core technology using variable impedance actuators.

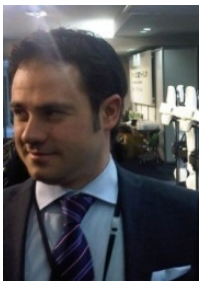

Nicola Vitiello received the M.Sc. degree in biomedical engineering (cum laude) from the University of Pisa, Italy, in 2006, and from Scuola Superiore SantAnna, Pisa, Italy, in 2007. He also received the Ph.D. degree in biorobotics from the Scuola Su-

periore Sant'Anna, Pisa, Italy, in 2010. He is currently an Assistant Professor with The BioRobotics Institute, Scuola Superiore SantAnna, where he leads the Wearable Robotics Laboratory. He is the author or co-author of 20 ISI/Scopus papers and 30 peer-review conference proceedings papers. He has served as the Scientific Secretary of the EU FP7 CA-RoboCom project, and he is currently the Project Coordinator of: the EU FP7 CYBERLEGs Project, the IUVO Project funded by Fondazione Pisa, and the EARLYREHAB Project funded by Regione Toscana.

Dirk Lefeber received the degree in Study of Civil Engineering at the Vrije Universiteit Brussel and a PhD in Applied Sciences, Vrije Universiteit Brussel, in 1986. Currently he is professor at the dept. of Mechanical Engineering and head of the Robotics and Multibody Mechanics Research Group, Vrije Universiteit Brussel. His research interests are new actuators with adaptable compliance, dynamically balanced robots, robot assistants, rehabilitation robotics and multibody dynamics.